Memorias del XVI Congreso Latinoamericano
de Control Automático, CLCA 2014
Octubre 14-17, 2014. Cancún, Quintana Roo, México

Experimental Validation of Vision-Based System for the Characterization of Human Standing

Raul Chavez-Romero*, Antonio Cardenas*,Mauro Maya*
Karinna M. Vernaza and Davide Piovesan****

*Universidad Autónoma de San Luis Potosí, SLP, 78290, México;
(e-mail:raulcr2010@gmail.com,antonio.cardenas, mauro.maya@uaslp.mx).
**Gannon University, Erie, PA 16501 USA (e-mail:
[vernaza001, piovesan001]@gannon.edu)

Abstract: The need to understand the control strategies utilized by humans in their everyday activity requires the measurement of several variables which pertain to different aspects of the interaction with the environment. Most often these measurements can be grouped as kinematic, dynamic and biological-feedback variables. Hence, there is a strong need for the acquisition, analysis and synchronization of the information measured by a variety of transducers. We created a sensor-fusion suite for the acquisition of biometric information that can be used for the estimation of human control strategy in a variety of everyday tasks. This work focuses on the experimental validation of the integrated motion capture sub-system based on raster images. The system was able to capture the complex dynamics of a flexible robot by means of two inexpensive web cameras. Finally, modelling quiet standing of humans as a second order inverted pendulum the instrumental setup was used to estimate the parameters that characterize the system during a recovery from a fall.

Keywords: Raster Image, Force Sensor, Balance, Posture, Stiffness, Stability.

1. INTRODUCTION

As the ageing population grows and life expectancy increases, postural stability is becoming a critical issue. As people age, their risk of falling and injury themselves increases particularly after age 65. It has been reported that 1/3 to 1/2 of the older population experiences a fall every year (Janssen, Samson, & Verhaar, 2002). Is reported that the number of deaths related to accidental fall in people more than 80 years old is comparable to the number of deaths caused by motor vehicle accident in the population between 15 to 29. Hip fracture is among the most common injury related to falls. Two third of such population are women (Langlois, et al., 1998) given their tendency to osteoporosis. This type of injury imposes a long period of immobilization where older individuals lose their autonomy. Although surgeries to repair fractures are straightforward and relatively simple fixes, complications after surgery can be dangerous to the point that 1/3 of these patients died in one year after surgery (Da Silva Gama & Gómez-Conesa, 2008).

Understanding the mechanisms involved in postural stability is indispensable to get a better knowledge of the way the human body can regain balance against possible disturbances. Postural stability requires the ability to modulate the position of the body's centre of pressure to react to the movement of the centre of gravity. Unexpected perturbations that displace the centre of gravity of the subject are one of the leading causes of fall.

Given the importance of the problem, the study of the different strategies that humans use to maintain postural stability is paramount. The problem is usually approached by establishing a relationship between the position of the center of pressure (COP) and the position of the center of gravity (COG). The former measurement is usually attained from force measurements obtained with a force plate and a set of force transducers. The latter is obtained by estimating the inertia of the subject's body segment parameters and tracking the movement of some anatomic landmark via a motion capture system. While force transducers are relatively affordable even for small businesses, the acquisition of motion capture systems is often prohibitive, especially for cost savvy enterprises. Thus, creating an affordable, yet accurate, integrated apparatus able to estimate both the position of the center of pressure and the position of the center of gravity would be beneficial for the study of postural stability.

We designed and built a new system that integrates a commercial force-plate with a custom made motion capture system using two webcams and custom made software programmed in Matlab. This work presents a static and dynamic calibration of the apparatus using a flexible robot test-bed.

2. METHODS

2.1 Hold and Release Paradigm

The hold and release paradigm (H&R) is a technique to perturb the quiet standing of an individual, with the scope of exciting a neuro-mechanical response against falling (Bortolami, DiZio, Rabin, & Lackner, 2003). Figure 1 illustrates the paradigm in detail. In phase A the subject is in

quiet standing and s/he is generating a torque at the ankle to counteract the torque generated by gravity as the center of mass is slightly forward with respect to the pivoting point at the ankle. In phase B the experimenter applies a steady force,

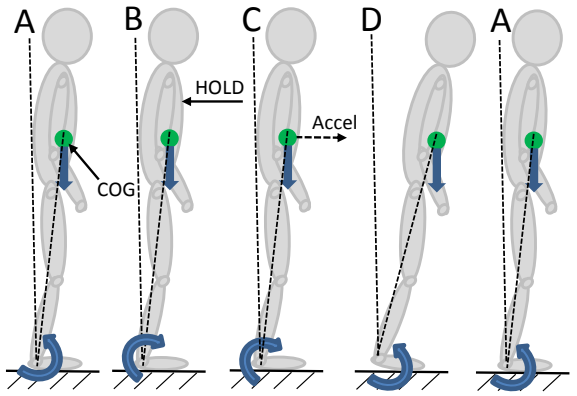

Fig. 1 A) Quiet standing. B) Hold. C) Release with consequence acceleration of the center of mass forward. D) Recoil where fall is prevented and quiet posture is regained as in condition A.

to the subject's sternum as to push her/him backwards. Hence, the subject produces a torque at the ankle to counteract the external load, which generates a torque around the same pivoting point. When the external load is suddenly removed in phase C the torque that was exerted by the subject to counteract the external load drives the body forward. In phase D the fall is halted by the reaction of the neuro-mechanical systems through the application of a counteracting torque at the ankle. This is the instant after which the time series describing the position of the COG can be used in a system identification algorithm to identify the properties of human balance. Indeed, the subject is at its largest displacement far away from the equilibrium position. At this point we can hypothesize that the central nervous system (CNS) imposes a desired position command to bring the COG back to the equilibrium position as fast as possible. The command, as a first approximation, can be assume to be a step. The error between the desired angular position θ_f and the actual position induces the generation of a torque at the ankle via the neural-controller. The torque is applied to the muscle-skeletal system which moves toward the desired equilibrium position (Fig.1D-A). Thus, after a transient response, posture is finally stabilized as it was in phase A.

Although Human body is a vibrational system with multiple DOFs and multiple modes and resonant frequencies; by analyzing the power spectrum of the response, more than 80% of the signal variance is described by the first mode so it make feasible to use the inverted pendulum model as a first approximation (Gage, Winter, Frank, & Adkin, 2004). Therefore in this paper the system is modelled as an inverted pendulum with one degree of freedom (DOF) (i.e. the rotation around the ankle). If a residual oscillation is present, the system is at least second order having two complex conjugated poles. The natural frequency ω_n can be estimated from the period of oscillation T_d of the COG before system stabilization according to the following formula:

$$\frac{2\pi}{T_d} = \omega_d = \omega_n\sqrt{1-\zeta^2} \qquad (1)$$

If the system is under-damped, the damping ratio ζ can be estimated from the over-shooting $\theta_{max} - \theta_f$, according to the following formula:

$$\frac{\zeta}{\sqrt{1-\zeta^2}} = \frac{1}{\pi} ln\left(\frac{\theta_f - \theta_0}{\theta_{max} - \theta_f}\right) \qquad (2)$$

where θ_{max} is the maximum angular displacement during phase D, θ_f is the desired angle at equilibrium in phase A, and θ_0 is the position at the end of phase C which is also the beginning of phase D (Fig.1-2).

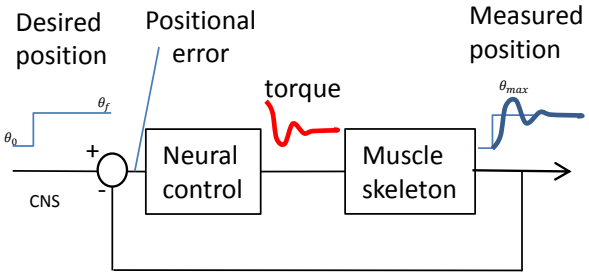

Fig. 2 Block diagram of positional step response from Phase D back to Phase A.

Even though a model that accounts for the mere torque generated at the ankle can describe the recovery of balance, the mechanism used by humans to control postural stability can be far more complex than the simple application of a torque at the ankle. The internal forces generated at the knee, hip, and spine are used to change body pose producing shear forces and changes in the center of pressure at the ground to make the COP move with respect to the COG in a desired manner.

2.2 Hardware Description

The apparatus to capture the H&R paradigm requires a system that measures the ground reaction forces and a system able to track the continuous change in position of the subject's center of mass. We used a commercial force plate (AMTI Accugait) to measure the ground reaction forces and developed an integrated vision system to track the subject's center of mass position. Both measuring systems were wired to a desktop computer with Intel Core 2 Duo processor at 2.33GHz, 2.00GB of RAM memory, and 64-bit Windows 7 Professional edition. As it can be seen by the computer's specifications, a powerful computer is not needed. We used a raster image acquisition system composed of two USB webcam Logitech c170 with definition of 640x480. The analysis and software interface was developed using Matlab 7.12.0.

Furthermore, to test the accuracy of the measurements we calibrated the camera-based tracking system against a robotic device as described in the following sections.

2.3 Robotic Device

The robotic device that we used was a modification of the ECP 505 inverted pendulum. The ECP 505 consists of a pendulum rod which supports a boom consisting of a sliding

Table 1. Pendulum Parameters

Definition	Sym	Value
Length of pendulum rod to sliding rod T section	l_0	0.33m
Mass of the sliding rod including all attachment elements	m_1	$m_{10}+ m_{w1}$
Mass of sliding rod with belt, belt clams and rubber guards but without brass doughnuts counterweight	m_{10}	0.103kg
Weight of combine brass doughnuts counterweight	m_{w1}	0.11kg
Mass of complete assembly minus m_1	m_2	$m_{20}+ m_{w2}$
Mass of brass balance counterweight	m_{w2}	1kg
Mass of complete assembly minus m_1 and m_{w2}	m_{20}	0.785kg
Position of COG of complete pendulum assembly with the sliding rod and counterweight removed	l_{co}	0.071m
Mass Moment of inertia with respect to pivot when m_{w2}=0	J_o*	0.0246kg m^2
Position of counterweight COG	l_{w2}	-0.14m

balance rod. A DC servo motor, positioned at the lower extremity of the pendulum rod, is used to drive the sliding balance rod through a drive shaft. The shaft is connected via a gear to a toothed belt which tension is regulated by two dead end pulleys. This sliding rod is moved horizontally to control the vertical pendulum rod. A brass counter weight can be added to the pendulum rod to alter the system's COG. Two encoders are used to track the position of the sliding rod and the pendulum rod: the first is collinear with the servo axis; the second is located at the pivoting point. The mass and position of COG for the various element of the device are illustrated in Table 1 (Chanchareon, Sangveraphunsiri, & Chantranuwathana, 2006).

The device was modified by adding a flexible rod of known stiffness to the pendulum rod whose characteristics are illustrated in Table 2. This flexible contraption was added in order to better approximate the experimental condition of a human experiment. Indeed, the tip of the robotic arm would coincide with the position of an averagely built individual's COG, which is usually located approximately in front of the second sacral vertebra (Franklin, 2012). The system as modified reflects two main characteristics of human standing which are: i) a pivoting point at the base representing the ankle to simulate a scaled stiffness of the human flexible joint, and ii) the flexible rod integrated with the pendulum can effectively model the flexibility of the human spine and hip joints. Hence the device can be defined as a robot with both one flexible joint and one flexible link (Fig. 3).

2.4 Pinhole Camera Model and Estimation of 3D points

A linear relationship between points in three dimensional space and its projections in a plane can be established based on the pinhole camera model. The mapping corresponding to the pinhole camera model is defined by a matrix P $[3 \times 4]$ formed by scalars, which has only 11 degrees of freedom (DOF) (Zhengyou, 2000). The P matrix can be decomposed in the following form:

$$P = KR[I \mid -D] \tag{3}$$

Table 2. Flexible Rod Parameters

Position flexible rod COG	l_{w3}	0.711m
Mass of the flexible rod	m_3	0.013 kg
Young modulus of the flexible rod	E	78.8 GPa
Geometric moment of inertia of cross sectional area	I	3.3e-11 m^4
Mass moment of inertia with respect to the rod end	J_{rod}	0.022 kg m^2

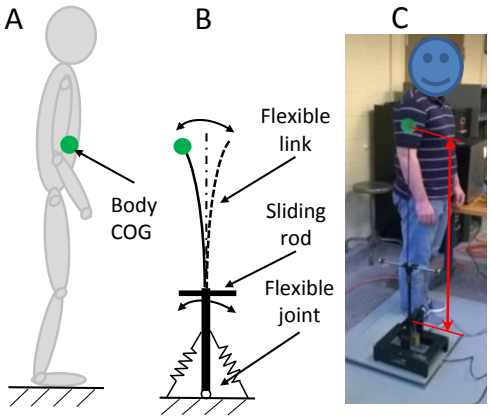

Fig. 3. A) Segmental model of human standing. B) Analytical schematic of robot. C) Human and robotic device proportions.

where I is the 3×3 identity matrix, D is the center of the camera with respect to a world reference frame, R is a rotation matrix in 3D, and K is the calibration matrix:

$$K = \begin{bmatrix} \alpha_x & S & p_x \\ 0 & \alpha_y & p_y \\ 0 & 0 & 1 \end{bmatrix} \tag{4}$$

where α_x and α_y correspond to the focal distance multiplied by an adjustment factor to consider the possibility that the sensor cells of the camera (CCD for example) are not squared, p_x and p_y are the coordinates of the principal point (center of the image) and S is the skew factor, which is zero if the axis of the sensor are orthogonal (normal case). The matrix K has 5 DOF and the matrices R and D have 3 DOF each summing up to a total of 11 DOF P.

The relationship between the point in $3D$ space and its projection in the image is well known and it is given by the following equation (Hartley & Zisserman, 2003):

$$\begin{bmatrix} x \\ y \\ 1 \end{bmatrix} = \begin{bmatrix} p_1 & p_2 & p_3 & p_4 \\ p_5 & p_6 & p_7 & p_8 \\ p_9 & p_{10} & p_{11} & 1 \end{bmatrix} \begin{bmatrix} X \\ Y \\ Z \\ 1 \end{bmatrix} \tag{5}$$

where $[x, y]^T$ is the point in the image and $[X, Y, Z]^T$ is the point in the world reference frame. Equation (5) can be rewritten as a linear system in the following manner:

$$\begin{bmatrix} X & Y & Z & 1 & 0 & 0 & 0 & 0 & -xX & -xY & -xZ \\ 0 & 0 & 0 & 0 & X & Y & Z & 1 & -yX & -yY & -yZ \end{bmatrix} \mathrm{P} = \begin{bmatrix} x \\ y \end{bmatrix} \tag{6}$$

To calculate the matrix P at least 6 points are required $(i = 1,2,\ldots,6)$ However, 5 points and the coordinate x or y of the sixth point are enough to find the analytical solution of the 11 parameters of vector P. If more than 6 points are used in computing P, an over constrained system is obtained and a minimization process is required to yield the solution. An over constrained system produces better results when estimating the vector P in the sense that the minimization process average out the white noise in the estimation of the P parameters if the data number is large and the visual cues are located widely spread on the image plane.

Once the P parameters, have been obtained for at least two participating cameras, the target point $[X \quad Y \quad Z]^T$ can be estimated by solving the once redundant set of equations:

$$\begin{bmatrix} x^j \\ y^j \end{bmatrix} = \begin{bmatrix} p_1^j & p_2^j & p_2^j & p_4^j \\ p_5^j & p_6^j & p_7^j & p_8^j \end{bmatrix} \begin{bmatrix} X \\ Y \\ Z \\ 1 \end{bmatrix} for\ j = 1,2 \quad (7)$$

Where (x^j, y^j) represent the sampled camera-space location of the target point on camera j.

2.5 Graphical User Interface

To calibrate the vision system two cameras are positioned in two different fixed locations. Furthermore a set of objects whose location is known in space is also required. For this experiment we use a set of checkerboard patterns, with black and white squares of 30 mm x 30 mm (Fig. 4).

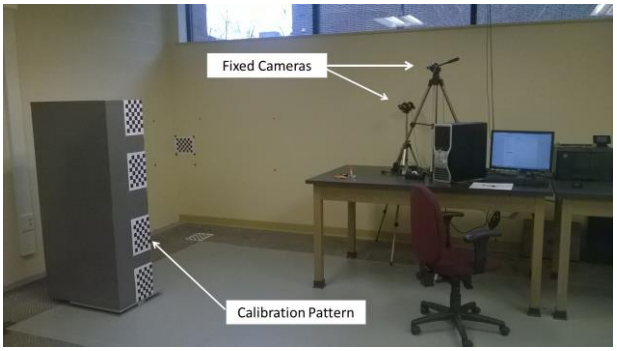

Fig. 4. Settings for calibrations pattern for estimation of vision parameters.

To compute and test the calibration parameters P, a Matlab program with a Graphical User Interface (GUI) was developed. The interface is used to monitor each camera either as a video or as a static image. The calibration can be done manually by clicking on the same physical point represented in each camera images. This allows an easy identification of the pixel coordinate in each camera image corresponding to the physical point in Cartesian space. After the data-points set has been acquired the vision parameters of section (2.4) can be calculated using a button on the GUI. After obtaining the camera parameters it is possible to test the accuracy of the system by selecting more points in the pictures whose location is known in the physical space and evaluate the error between the estimated position and the known position in the physical space.

3. EXPERIMENTS

3.1 Static Calibration

To obtain the P parameters a black and white checkerboard pattern was used, the grid was 88 X 88 divisions, each square was 30 mm X 30 mm. A total of 188 corners of the imaged squares were obtained by each camera.

As explained in section 2.4, the P parameters were estimated based on the point locations of n corners of a checkerboard pattern. To assess the accuracy of the P parameters and the overall precision of this vision system, the P parameters were computed using only (n-1) points out of the n original points, the 3D position for the i^{th} point, which was left out from the n data points, was estimated. Then, an error was defined as the Euclidean distance between the actual 3D position of the point and its estimated position by the vision system so that an error was associated to that point. This process was repeated for all 188 points. The average error for all 188 points was 1.89 mm with a standard deviation of 0.95 mm. The separation distance between the cameras and the calibration pattern was about 2.5 m and the pixel resolution was 4 mm/pixels which correspond to 0.2 degrees of angle resolution. Note that due to the least square regression described in section 2.4 it is possible to reach sub-pixel accuracy. With these results it was possible to conclude that a high profile camera for vision-machine applications was not required and off-the-shelf webcams with a 640 X 480 pixels resolution provide enough accuracy to estimate 3D on a camera scene.

The system was also calibrated against a machine vision camera system (uEye) where comparable results were obtained. Anyhow additional validations are necessary for the calibration of the system against an active or passive marker commercial motion capture system.

3.2 Experimental validation on robot

The robotic device gives us the possibility to impose a known trajectory to the pendulum rod and therefore verify if position tracking can be achieved. The ECP 505 is an under actuated mechanism controlled via the movement of the sliding bar. It is possible to impose a known movement to the sliding bar and design a controller in order to attain its desired trajectory. However, due to the couple dynamics of the system, the trajectory of the sliding bar induces an angular trajectory of the pendulum rod which can be measured via the encoders positioned at the pivoting point, and therefore actively controlled.

To validate the performance of the vision system, tracking of a movement of a tip of a pendulum was executed. A visual marker was placed on the tip of flexible bar and a position profile was executed by a PD controller on the pendulum. The measurement was done on a single plane; however having two cameras facilitate their positioning. Indeed, two cameras can acquire any plane in 3D independently of the subject position. Thus, when the static calibration is done the cameras do not need to be relocated in order to be precisely aligned with a plane parallel to the movement.

We imposed a position step to the sliding rod equivalent to an amplitude of 6º. This amplitude was chosen as it produces an angular displacement of about 8º on the pendulum rod compatible with the angular deviation from the ankle pivoting point of the human COG during H&R paradigm experiments in unimpaired individuals. The rising trajectory of the step from 0º to 6º was modulated using a cubic trajectory (i.e piecewise constant jerk) were the change in acceleration time was fixed to 500ms.

A green circular marker was used as visual cue to identify the desired target point. This visual marker was attached to the tip of the flexible bar. This marker was identified on camera space in both cameras by filtering the green marker and by computing the centroid of the detected spot on camera space. The robot was positioned on the force platform as a mean to identify the reaction forces generated by the change of the COG physical location. Once the P parameters were established and the camera-space location of the COG point was found in each of the two cameras, it was possible to estimate the 3D coordinates of the COG.

During the execution of the motion, a video was acquired at 10 fps. The visual mark on the tip of the pendulum was detected by both cameras and their corresponding 3D location was estimated by using its camera point location in each image as explained in section 2.4.From this estimated tip location of the pendulum its corresponding angle position at each instant with respect to the known pivoting point was computed as the corresponding angle to the subtended arc of the pendulum tip between two consecutive instants. Even thought there is a delay between the acquired images between both cameras of the order of 0.04 seconds in average, it is not significant to the response of the system and it can be neglected.

3.3 Hold and Release Experiment on Human

After validating the vision based system we applied a similar experimental protocol on one unimpaired individual in order to estimate the response to the H&R paradigm.

The subject position her/himself on top of the force platform in a natural posture. The experimenter pushed the subject on the sternum while the subject tried to resist the perturbation. Hence a sudden release triggered the control reaction for recovering falls while the position of the COG was recorded by the vision based system and the total torque exerted at the point of contact with the ground was recorded via the force plate.

4. RESULTS

4.1 Response to a Positional Step on robot

The error between the commanded angle by the controller of the ECP 505 and the assessed angle by the vision system was in average less than 1 degree with a standard deviation of 0.36 (Fig 5). We can also notice a residual high frequency oscillation of the angular displacement tracked by the vision system. This oscillation was expected due to the flexibility of the rod. Thus, we can prove that even if higher dynamics are present in the system, the tracking of a step function response with a displacement of 8º can be tracked by our vision system

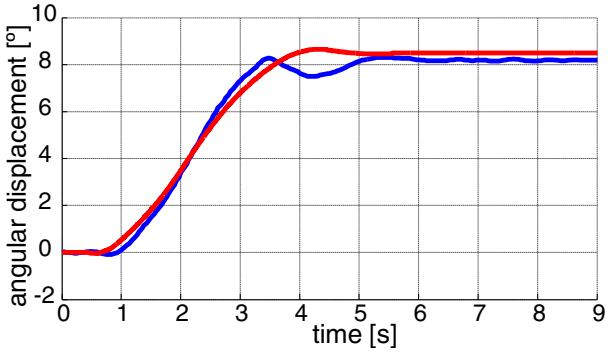

Fig. 5 Tracking angle from vision system (blue) and tracked angle of a pendulum using the robot's encoder (red).

4.2 Response to Hold and Release in human

In Fig. 6 we can observe both the total torque recorded by the force plate and the movement of the center of mass. Notice that the in the graphs 0 torque corresponds to the residual torque in Fig 1-a, and 0 angle correspond to θ_f. We can hypothesize that the torque is the variable directly commanded by the neural-controller and that the movement of the COG (bottom panel) is a direct consequence of the torque applied to the physical system to stabilize it. We can observe that when the subject COG reaches the absolute maximum displacement (-6º circa) we are at the beginning of the recoil phase (Fig. 1D). From this point on, the condition is equivalent to a step in position as described in section 2.1 The control system is reacting to drive the system back to its original equilibrium position. Thus, by observing the angular displacement graph we can have an idea of the general characteristics of the system. We can start from the assumption that the system is second order, since it is known to have inertia. This is confirmed by observing 1) that there is a residual vibration which can come only from a double pole of complex nature and 2) that the shape of the rising trajectory during the recoil phase shows that the curve cannot be approximated by a straight line in the neighborhood of the initial condition. We can also observe that the system overshoots the threshold of 0º, suggesting that the system is under-damped.

If we assume the system to be a single inverted pendulum commanded at the ankle, we can measure the main period of oscillation in Fig. 6, bottom panel. The time between the highlighted signal peaks is 5s. Thus, the damped resonance frequency of the system is 0.25Hz (see Equation 1). The damping ratio estimated using Equation 2 by Fig. 7 is 0.22 which bring a natural frequency of 0.256Hz. These parameters can give a useful quantitative measure of the capability of a human to prevent fall and might be employed as a quantitative scale.

5. DISCUSSION

In the shaded part of Fig 6 bottom panel, it is noticeable that the torque exerted at the ankle is still slightly positive. This is because in phase B of Figure 1 the force applied by the experimenter created a moment that did not overcome the

whole moment created by gravity on the center of mass. Hence, the subject can drastically reduce the torque that s/he needs to exert to counteract gravity. The subject therefore was not forced to push against the experimenter as gravity was of help. Nevertheless, after the sudden release a negative torque is instantly generated due to the forward movement of the center COG that require a generation of torque at the ankle to recover balance. In this phase we can see a positive peak of the angle, most likely created by the subject pushing the hips forward and the shoulder back. This postural adjustment would give more time (due to a larger positional excursion) to invert the sign of the torque which reach its negative peak θ_0 at the beginning of phase D.

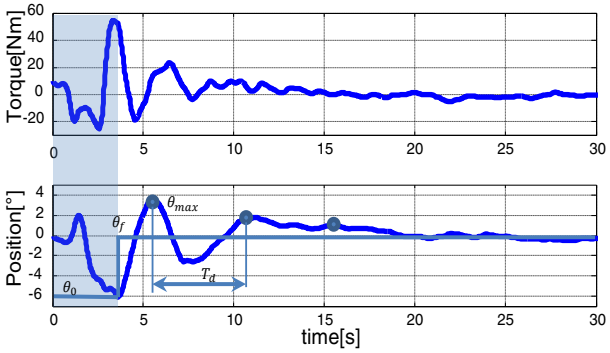

Fig. 6 Torque trajectory at the ankle and angular displacement of the COG for the experiment on one unimpaired individual. (Top panel) Measurement from force plate of the total torque at the ground. (Bottom panel) position of the center of gravity as tracked by the vision system. Shaded area indicates phases B and C from Fig 1. Non shaded area represents the transient in the recovery of fall between phase D and phase a in Figure 1. T_d *is the period of oscillation of the COG before system stabilization;.* θ_{max} *is the maximum angular deviation during phase D,* θ_f *is the desired angle at equilibrium in phase A, and* θ_0 *is the position at the beginning of phase D.*

The initial compensatory phase where the hip are pushed forward cannot be measured directly but we can observe that there exist at least two frequencies at which the system oscillates during the stabilizing phase around the aforementioned threshold, suggesting that the system has at least 2 dominant modes. Further studies are necessary to address the capability of our instrumentation to estimate the parameters of more complex systems in more detail.

6. CONCLUSIONS

The sensor fusion suite that we devised consists in a centralized program that can synchronize and integrate the information coming from several transducers. Up-to-date the system can combine a set of two USB web-cameras and a six degrees-of-freedom force platform. The cameras utilize a vision algorithm that transforms the markers coordinates acquired in camera space to a coordinates in Cartesian space using a linear camera model. Furthermore, a biomechanical model of the human is integrated in the system for the reconstruction of the tracked movements in the joint space. The information from the joint angular displacements together with information from the force platform can then be utilized to estimate the dynamic behavior of the recovery to prevent falls. The architecture of the systems allows for the integration of transducers beyond those implemented to-date, including inertial measurement units, electromyography and pressure sensors.

By monitoring the natural frequency of the inverted pendulum it is possible to estimate the stiffness at the joint. An increase in natural frequency (with similar inertia) implies an increase in stiffness and a consequent increase of the margin of stability of the control system. Thus, an increase in the margin of stability compared to normative data indicate a compensation strategy that should be carefully monitor as it might indicate that the subject is more prone to fall.

The information acquired by our suite can be readily integrated with neuro-mechanical simulation of quiet standing. The system can monitor the interaction of the whole body with external force perturbations and is particularly suited for the estimation of internal variables such as stiffness and damping. These parameters are particularly important when a comparison can be made between control subjects and individuals who have been impaired as a consequence of injuries or neurological diseases, or are elderly and more prone to fall.

REFERENCES

Bortolami SB, DiZio P, Rabin E, & Lackner JR. Analysis of human postural responses to recoverable falls. Exp Brain Res 2003;151:387-404.

Chanchareon R, Sangveraphunsiri V, & Chantranuwathana S. Tracking Control of an Inverted Pendulum Using Computed Feedback Linearization Technique. Robotics, Automation and Mechatronics, 2006 IEEE Conference on. 2006. p. 1-6.

Da Silva Gama, Z. A., & Gómez-Conesa, A. Risk factors for falls in the elderly: systematic review. Rev Saúde Pública 2008; 42(5): 946-56.

Franklin EN. Dynamic alignment through imagery. 2nd ed. Champaign, IL: Human Kinetics; 2012.

Gage, W. H., Winter, D. A., Frank, J. S., & Adkin, A. L. Kinematic and kinetic validity of the inverted pendulum model in a quiet standing. Gait and Posture 2004; 9:124-132.

Hartley R, & Zisserman A. Multiple View Geometry in Computer Vision. Cambridge University Press; 2003.

Janssen HC, Samson MM, & Verhaar HJ. Vitamin D deficiency, muscle function, and falls in elderly people. The American Journal of Clinical Nutrition 2002;75:611-615.

Langlois J, Visser M, Davidovic LS, Maggi S, Li G, & Harris TB. Hip fracture risk in older white men is associated with change in body weight from age 50 years to old age. Archives of Internal Medicine 1998;158:990-996.

Zhengyou Z. A flexible new technique for camera calibration. Pattern Analysis and Machine Intelligence, IEEE Transactions on 2000;22:1330-1334.